

## Seismic Slip and Down-Dip Strain Rates in Wadati-Benioff Zones

MICHAEL BEVIS

The rate of accumulation of seismic moment in Wadati-Benioff zones is used to estimate strain rates in subducting slabs that are sinking through the asthenosphere. Between depths of 75 and 175 kilometers a typical down-dip strain rate is about  $10^{-15}$  per second, which implies that slabs in this depth range typically accumulate strains of order  $10^{-1}$ . This result is in accord with geometrical arguments that subducted slabs must experience large membrane strains to deform to their observed shapes. Mantle seismicity (repeated catastrophic shear failure) is apparently a primary mechanism by which large membrane strains accumulate in the cold cores of subducting slabs. Slabs are penetratively deformed, and they have low flexural rigidity compared to oceanic plates at the earth's surface.

ALTHOUGH SUBDUCTED SLABS OF lithosphere have been modeled as flexible but inextensible membranes (1) and as stiff elastic shells (2), the shapes of Wadati-Benioff zones (WBZs) suggest that slabs sinking through the upper 150 km of mantle commonly accumulate membrane strains of order  $10^{-1}$  (3–5). This implies a strain rate of order  $10^{-15} \text{ s}^{-1}$ , which approaches the strain rates associated with viscous flow of the asthenosphere (6). Lithospheric slabs are too cold in this depth range (7) to achieve this high a strain rate (throughout their thickness) by viscous flow (8). Detailed studies of focal mechanisms and hypocenter distributions suggest that mantle earthquakes are generated during catastrophic shear failure (9, 10). Because WBZs can be divided into large subregions in which down-dip compression or down-dip tension is the dominant focal mechanism (11, 12), the down-dip component of strain associated with mantle seismicity must accumulate with time. Therefore, seismic slip may provide a mechanism by which large membrane strains accumulate in the cold core of a subducting slab. I show that the cumulative seismic moment per unit time can be used to estimate the typical down-dip strain rate achieved by seismic slip in subducted lithosphere.

Seismic moment is a measure of the "size" of an earthquake (13, 14). It is defined by the equation

$$M_o = dS\mu \quad (1)$$

where  $d$  is the average displacement or slip on the earthquake's fault plane,  $S$  is the

area of the fault plane, and  $\mu$  is the rigidity of the surrounding rock. If the displacement on a major fault zone is achieved by seismic slip that is distributed uniformly over the area,  $A$ , of the fault, and the slip vector for each earthquake is parallel to the long-term slip vector on the fault, then the average slip,  $u$ , that accumulates during a sufficiently long time interval,  $T$ , is related to the cumulative seismic moment,  $\Sigma M_o$ , by Brune's (15) relation

$$u = \Sigma M_o / \mu A \quad (2)$$

Brune (15) and others (16) have used this relation to show that shallow earthquakes that are caused by underthrusting at several subduction zones yield a seismic slip rate that is comparable in magnitude to the average rate of plate convergence. A similar relation can be used to estimate intraplate strains achieved by intraplate seismicity (17). Consider a part of a subducting plate in which intraplate seismicity is uniformly distributed (Fig. 1). Let the down-dip length of the seismogenic volume be  $D$ , its along-strike length be  $L$ , and its thickness be  $t$ . I assume that each earthquake has a fault plane that is oriented such that the direction of maximum shortening (or lengthening) is down the dip of the plate. The average change in the down-dip length of the slab,  $\delta$ , for a time interval,  $T$ , characterized by cumulative seismic moment,  $\Sigma M_o$ , is given by

$$\delta = \Sigma M_o / 2\mu tL \quad (3)$$

Whereas Eq. 2 is derived by averaging and time-integrating coseismic slip over the area of a fault plane, Eq. 3 is derived by averaging and time-integrating the down-dip component of coseismic slip over a seismogenic volume. The average down-dip strain,  $\epsilon$  (which equals  $\delta/D$ ), for this time interval is

$$\epsilon = \Sigma M_o / 2\mu V \quad (4)$$

where  $V$  equals  $tLD$ , the volume of the seismogenic zone. The corresponding strain rate,  $\epsilon'$ , is simply

$$\epsilon' = \epsilon / T \quad (5)$$

The seismic moment of an earthquake is simply related (18) to its magnitude or its seismic energy release,  $E_s$ ; therefore, plots of worldwide seismic energy release (in various depth intervals) versus time for this century (14, 19) can be used to estimate the rate of accumulation of seismic moment. For shallow (interplate) underthrusting earthquakes,  $M_o$  is  $\sim 2 \times 10^4 E_s$ , whereas  $M_o$  is  $\sim 1.3 \times 10^4 E_s$  for mantle earthquakes in the depth range of 75 to 175 km. Seismic moments vary from about  $10^5$  Newton-meters (N·m) for small earthquakes to about  $10^{23}$  N·m for great earthquakes. The worldwide annual cumulative seismic moment is dominated by the timing of rare great earthquakes, and as a result the cumulative seismic moment has fluctuated from year to year by more than two orders of magnitude during this century (14). It is thought that the average rate of accumulation of seismic moment during this century adequately characterizes tectonic processes at the 1-million-year time scale, however (15, 16). The following order of magnitude calculation is presented to illustrate and support this contention.

Ocean floor is created at mid-ocean ridges at a rate close to  $3.5 \text{ km}^2 \text{ year}^{-1}$  (20) and destroyed at an equal rate at a system of deep sea trenches, which have a total length of about 40,000 km. This implies an average subduction rate close to  $87 \text{ mm year}^{-1}$ . Much if not all of this convergence is achieved by seismic slip at interplate thrust faults. The cumulative seismic moment that

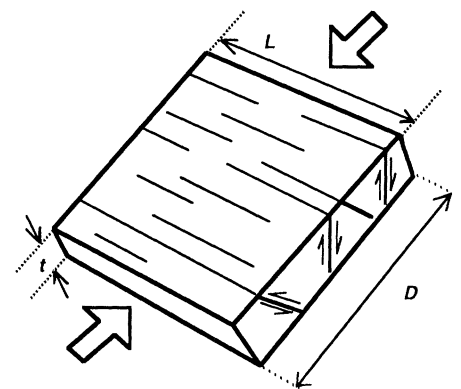


**Fig. 1.** A schematic depiction of the model used to compute down-dip strain rates within WBZs, showing the key geometrical parameters. The seismogenic part of the slab is uniformly penetrated by active faults, which are oriented such that the direction of maximum shortening (or lengthening) is down the dip of the slab. For purposes of illustration the slab is assumed to be under down-dip compression.

Department of Marine, Earth, and Atmospheric Sciences, North Carolina State University, Raleigh, NC 27695-8208.

was associated with shallow seismicity from 1904 to 1974 was  $\sim 6.4 \times 10^{23}$  N·m (19). About 95% of this moment was associated with seismicity in interplate thrust faults. The typical down-dip length of the seismically active interplate thrust fault is about 75 km. Subduction zones have a combined length of about 40,000 km, and therefore the seismicity that manifests interplate thrusting is distributed over a total area of about  $3 \times 10^{12}$  m<sup>2</sup>. For  $\Sigma M_o$  equal to  $\sim 6 \times 10^{23}$  N·m,  $A$  equal to  $3 \times 10^{12}$  m<sup>2</sup>, and  $\mu$  equal to  $3 \times 10^{10}$  N m<sup>-2</sup>, Eq. 2 yields an average slip  $u$  of  $\sim 6.7$  m. This value corresponds to an average seismic convergence rate of  $\sim 94$  mm year<sup>-1</sup>, which is in close accord with the average rate of plate convergence stated above. The derived seismic convergence rate is only an order of magnitude estimate; therefore, the excellent agreement is somewhat fortuitous. (The seismic convergence rate should underestimate the plate convergence rate because some plate convergence is accomplished aseismically.) This exercise does support the assumption that cumulative seismic moments derived from catalogs of large earthquakes can be used to estimate plate tectonic subduction rates, at least to an order of magnitude.

I now estimate strain rates in WBZs. I consider mantle seismicity in the depth range from 75 to 175 km, because in this region the geometry of WBZs is easily characterized, the contrast in mechanical strength between the subducting slab and the adjacent mantle is presumably a maximum, and the analysis is not complicated by the presence of a major phase transition. In this depth range, nearly all WBZs are dominated by earthquake focal mechanisms that indicate either down-dip compression or down-dip tension (11, 12). [The double WBZ beneath Japan is a clear exception because the upper zone is in down-dip compression and the lower zone is in down-dip tension (21). In the following order-of-magnitude calculation I simply ignore this anomaly.] As a first approximation I assume that all WBZs in this depth range fall in one of two classes: (i) all earthquakes manifest exactly down-dip compression, and (ii) all earthquakes manifest exactly down-dip tension. Equations 4 and 5 are used to estimate a typical magnitude (worldwide) for the absolute value of the down-dip strain rate. (That is, data from both classes of WBZs are combined to determine a global average of the down-dip strain rate irrespective of the issue of down-dip compression versus down-dip tension.) During the 71-year period from 1904 to 1974, the total seismic energy that was released in the depth range from 75 to 175 km was about  $6 \times 10^{18}$  J

(19). This implies a cumulative seismic moment,  $\Sigma M_o$ , of  $\sim 8 \times 10^{22}$  N·m. The combined length ( $L$ ) of subducted slabs in the depth range of interest is about 40,000 km. Their average dip is close to 45°. The WBZ typically has a thickness close to 30 km. Setting  $L$  equal to 40,000 km,  $t$  equal to 30 km,  $\mu$  equal to 60 GPa,  $D$  equal to  $100\sqrt{2}$  km, and  $T$  equal to 71 years, Eqs. 4 and 5 yield an average absolute strain rate,  $\langle |\dot{\epsilon}'| \rangle$ , of  $\sim 2 \times 10^{-15}$  s<sup>-1</sup>.

This estimate can be refined. In reality, in any WBZ there is some scatter of the stress axes associated with individual earthquakes about the down-dip direction (11, 12). Apperson and Frohlich (12) examined the focal mechanisms of 465 intermediate depth earthquakes and showed that about 50% of these events have either a P axis or a T axis lying within 31° of the down-dip direction. This scatter of stress axes about the down-dip direction means that the value above is an overestimate of the down-dip strain rate because only the down-dip component of the coseismic strain associated with a given earthquake contributes to down-dip strain of the slab. The results of Apperson and Frohlich indicate that the average absolute down-dip strain rate is overestimated by about a factor of 2. A correction that accounts for the double WBZ beneath Japan is considerably smaller and can be neglected in this treatment. The typical down-dip strain rate in subducting slabs in the depth range of 75 to 175 km is thus  $\sim 1 \times 10^{-15}$  s<sup>-1</sup>. This figure is a global average; the variation in the intensity of seismic activity from zone to zone indicates that local seismic strain rates vary by more than one order of magnitude (22). Because it takes about 1.5 million years, on average, for a slab to sink through this depth range, the typical absolute magnitude of the total accumulated strain at 175 km depth is  $\sim 5\%$ .

Most estimates of strain rates in the asthenosphere, on the basis of numerical models of viscous flow (6, 23), are of order  $3 \times 10^{-14}$  s<sup>-1</sup>. Thus strain rates in the asthenosphere may exceed those in slabs that are sinking through the asthenosphere by less than one and a half orders of magnitude. Clearly the traditional concept of WBZ seismicity as a passive indicator of stress in an essentially coherent slab of lithosphere is inappropriate (3, 10). The changes in curvature imposed on a subducting slab, in large part caused by the pattern of mantle flow (23), require the generation of large strains ( $\sim 10\%$ ) in the slab (3, 24). These strains are achieved in the colder parts of the slab by the integrated effect of large numbers of catastrophic shear failures (earthquakes) within the WBZ. These calculations suggest that subducted slabs are penetratively de-

formed, have little flexural rigidity, and do not behave as elastic shells.

If subducting slabs are not rigid, several theoretical models of mantle flow in subduction zones may need to be modified to account for the progressive changes in slab shape. At some point, anelastic processes will begin to dominate the mechanical behavior of a subducting plate as it enters the subduction zone. It is not yet clear where this change occurs, but if it occurs near or above the trench, models of trench-forebulge morphology with elastic plates are inappropriate. A barrier to subduction at a depth of 680 km, as many researchers have conjectured, would cause intense buckling of a slab with low flexural rigidity. Such buckling has not been observed, which suggests that the barrier does not exist. The occurrence of large numbers of active faults within subducting slabs may also have implications for slab dewatering or for melting of the slab or overlying asthenosphere because faults may act as conduits for migration of fluids.

#### REFERENCES AND NOTES

1. F. Frank, *Nature* **220**, 363 (1968); X. Le Pichon, J. Francheteau, J. Bonin, *Plate Tectonics* (Elsevier, Amsterdam, 1973).
2. A. T. Smith and M. N. Toksoz, *Geophys. J. R. Astron. Soc.* **29**, 289 (1972); G. F. Davies, *J. Geophys. Res.* **85**, 6304 (1980); Y. Fukao, K. Yamaoka, T. Sakurai, *Phys. Earth Planet. Inter.* **45**, 59 (1987).
3. M. Bevis, *Nature* **323**, 52 (1986).
4. K. Strobach, *Z. Geophys.* **39**, 819 (1973); G. V. Burbach and C. Frohlich, *Rev. Geophys.* **24**, 833 (1986).
5. D. Giardini and J. H. Woodhouse, *Nature* **319**, 551 (1986).
6. D. L. Turcotte and G. Schubert, *Geodynamics* (Wiley, New York, 1982).
7. G. Schubert, D. A. Yuen, D. L. Turcotte, *Geophys. J. R. Astron. Soc.* **42**, 705 (1975).
8. R. Wortel, *Nature* **296**, 535 (1982).
9. Y. Fukao, *Phys. Earth Planet. Inter.* **5**, 61 (1972); S. Billington and B. L. Isacks, *Geophys. Res. Lett.* **2**, 63 (1975).
10. D. Giardini and J. H. Woodhouse, *Nature* **307**, 505 (1984).
11. B. L. Isacks and P. Molnar, *Rev. Geophys. Space Phys.* **9**, 103 (1971); M. S. Vassiliou, *Earth Planet. Sci. Lett.* **69**, 195 (1984).
12. K. D. Apperson and C. Frohlich, *J. Geophys. Res.* **92**, 13821 (1987).
13. K. Aki, *Bull. Earthquake Res. Inst. Tokyo Univ.* **44**, 23 (1966).
14. H. Kanamori, *Nature*, **271**, 411 (1978).
15. J. N. Brune, *J. Geophys. Res.* **73**, 777 (1968).
16. G. Davies and J. Brune, *Nature* **229**, 101 (1971); K. C. McNally and J. B. Minster, *J. Geophys. Res.* **86**, 4949 (1981).
17. W. M. Chapple and D. W. Forsyth, *J. Geophys. Res.* **84**, 6729 (1979).
18. H. Kanamori and D. L. Anderson, *Bull. Seismol. Soc. Am.* **65**, 1073 (1975).
19. K. Abe and H. Kanamori, *J. Geophys. Res.* **84**, 3589 (1979).
20. B. Parsons, *ibid.* **87**, 289 (1982).
21. A. Hasegawa *et al.*, *Tectonophysics* **47**, 43 (1978); B. L. Isacks and M. Barazangi, in *Island Arcs, Deep Sea Trenches and Back Arc Basins*, M. Talwani and P. Pitman, Eds. (American Geophysical Union, Washington, DC, 1977), pp. 99–141.
22. Strain rates vary with depth, too. The rate of accumulation of seismic moment in WBZs declines roughly exponentially with depth in the depth range

of 75 to 300 km. Both the number of events and the cumulative moment per unit depth decrease by about two orders of magnitude in this depth interval. In contrast, the total along-strike length of all subducted slabs decreases by less than one order of magnitude as depth increases from 75 km to 300 km. Therefore, the numerator of Eq. 4 decreases more rapidly with increasing depth than does the denominator, and as a result the (seismic) down-dip

strain rates in this depth interval tend to decrease with increasing depth.

23. B. Hager and R. J. O'Connell, *Tectonophysics* 50, 111 (1978).
24. Giardini and Woodhouse (5) argue that the Tonga slab has deformed by shear at a rate comparable to the one that I calculate.

24 December 1987; accepted 13 April 1988

## Bacterial Manganese Reduction and Growth with Manganese Oxide as the Sole Electron Acceptor

CHARLES R. MYERS AND KENNETH H. NEALSON

**Microbes that couple growth to the reduction of manganese could play an important role in the biogeochemistry of certain anaerobic environments. Such a bacterium, *Alteromonas putrefaciens* MR-1, couples its growth to the reduction of manganese oxides only under anaerobic conditions. The characteristics of this reduction are consistent with a biological, and not an indirect chemical, reduction of manganese, which suggest that this bacterium uses manganic oxide as a terminal electron acceptor. It can also utilize a large number of other compounds as terminal electron acceptors; this versatility could provide a distinct advantage in environments where electron-acceptor concentrations may vary.**

**M**ICROBIAL REDOX REACTIONS are important mechanisms for mobilizing metals and organic compounds in natural, anaerobic, aquatic environments. Important microbial reactions include those involving the oxidation of organic matter coupled to the reduction of nitrate ( $\text{NO}_3^-$ ), ferric iron [Fe(III)], manganese oxides [containing Mn(IV) and Mn(III)], or sulfate ( $\text{SO}_4^{2-}$ ), and the conversion of organic matter to carbon dioxide ( $\text{CO}_2$ ) and methane ( $\text{CH}_4$ ) (1).

Iron (2) and manganese may represent the primary electron acceptors for organic matter oxidation in sedimentary environments where they are enriched. In marine sediments, Fe and Mn reduction would likely be important in the zone between the region of oxygen removal and the region of sulfate reduction; in freshwater sediments, which are characteristically low in both  $\text{NO}_3^-$  and  $\text{SO}_4^{2-}$ , metal reduction would occur between the regions of oxygen depletion and  $\text{CO}_2$  reduction (methanogenesis).

Bacterially mediated Mn reduction can occur indirectly when reduced, metabolically excreted end products, such as sulfide (3) and certain organic compounds (4, 5), react abiotically with manganese oxides. Results from several studies (6-9), as well as thermodynamic considerations (10), suggest that some bacteria may link Mn reduction to the oxidation of organic substrates. Some bacteria have been shown to reduce Mn(IV)

under both aerobic and anaerobic conditions (6, 9). In contrast, Burdige and Nealson (7) suggested that certain bacteria could do this only under anaerobic conditions, but they did not work with pure cultures and were thus unable to identify the Mn-reducing microbes. We have isolated and characterized a bacterium that reduces Mn(IV) only under anaerobic conditions and couples its growth to this reduction.

The Mn-reducing bacterium *Alteromonas putrefaciens* strain MR-1 was isolated from the anaerobic sediments of Oneida Lake, New York. These sediments, although aero-

bic at the water-sediment interface, become anaerobic a few millimeters beneath the interface. During the summer months extensive Mn(IV) reduction occurs, which results in pore water Mn(II) concentrations of greater than  $100 \mu\text{M}$  and a rapid upward flux of Mn(II) into the lake water (11, 12).

We established enrichment cultures of the anaerobic sediments by the use of LO medium (13) with 0.75% agar, succinate or acetate as the carbon sources, and  $\text{MnO}_2$  (approximately  $1 \text{ mM}$ ) as the electron acceptor. These cultures were incubated at room temperature, and after a period of 2 to 7 weeks the  $\text{MnO}_2$  was reduced. Secondary enrichments were established from these cultures by use of the same LO medium. After the  $\text{MnO}_2$  in the secondary enrichments had been reduced, the cultures were transferred under anaerobic conditions (13) to agar plates of the LO medium containing an overlay of  $\text{MnO}_2$  in 0.75% agar. In less than 1 week, zones of visible reduction (that is, clearing) in the  $\text{MnO}_2$  top agar were evident; no visible colonies were noted in these zones, although MR-1 was repeatedly isolated in pure culture from such zones. MR-1 apparently stopped growing in an area after the local supply of  $\text{MnO}_2$  was depleted. This implies that MR-1, a motile bacterium that could move through the  $\text{MnO}_2$ -rich overlay, requires physical contact with insoluble  $\text{MnO}_2$  to grow. In contrast, if MR-1 mediated Mn reduction through the release of a diffusible reductant, then visible colonies within the zones of Mn reduction would be expected as is observed with sulfide-generating bacteria (3). We identified MR-1 as a strain of *A. putrefaciens* by conventional biochemical identification tests (14).

**Fig. 1.** Manganese reduction in liquid medium by MR-1. (A) Manganese reduction versus time for different numbers of cells: no cells ( $\square$ );  $9.33 \times 10^5$  cells  $\text{ml}^{-1}$  ( $\blacktriangle$ );  $1.87 \times 10^6$  cells  $\text{ml}^{-1}$  ( $\circ$ );  $3.73 \times 10^6$  cells  $\text{ml}^{-1}$  ( $\blacksquare$ );  $7.46 \times 10^6$  cells  $\text{ml}^{-1}$  ( $\triangle$ );  $1.49 \times 10^7$  cells  $\text{ml}^{-1}$  ( $\bullet$ ). Cell number was determined by colony counts on LB medium (21) with 1.5% agar. The concentration of  $\text{Mn}^{2+}$  was determined by the measurement of free  $\text{Mn}^{2+}$  and did not include  $\text{Mn}^{2+}$  that may have been bound to insoluble  $\text{MnO}_2$  (22). (B) Manganese reduction as a function of relative cell number; these data were obtained from (A). In three independent experiments, the y-axis intercept was equal to  $0.5 \pm 0.3 \mu\text{M}$ . (C) Temperature optimum of Mn reduction by MR-1 at pH 7.4; media at all temperatures contained  $6.36 \times 10^6$  cells  $\text{ml}^{-1}$ . (D) Optimum pH of manganese reduction by MR-1 at  $24^\circ\text{C}$ ; media at all pH values contained  $1.83 \times 10^6$  cells  $\text{ml}^{-1}$ . The net Mn reduction values in (C) and (D) were obtained by subtracting the values for Mn reduction in the absence of cells from reduction in the presence of cells. Experiments were conducted in LO medium (13) as described (23). The data shown in (C) and (D) were reproducible in duplicate experiments.

